

A mechanistic rationalization of unusual kinetic behavior in proline-mediated C–O and C–N bond-forming reactions†

Suju P. Mathew,^a Martin Klussmann,^a Hiroshi Iwamura,^{‡a} David H. Wells, Jr.,^{§a} Alan Armstrong^a and Donna G. Blackmond^{*ab}

Received (in Cambridge, UK) 12th July 2006, Accepted 10th August 2006

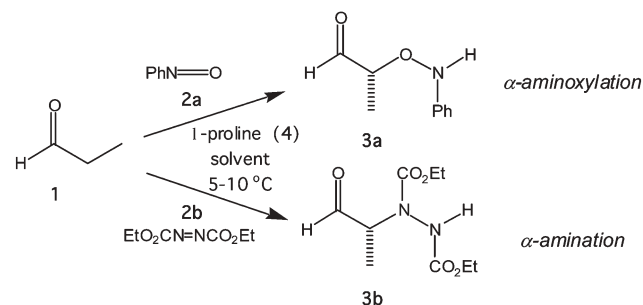
First published as an Advance Article on the web 31st August 2006

DOI: 10.1039/b609926b

Kinetic evidence supports the role of the reaction product in the catalytic cycle of proline-mediated α -aminoxylation and α -amination reactions, providing both design principles as well as a model for the evolution of efficiency in catalysis.

The demonstration by List *et al.*¹ in 2000 that proline mediates intermolecular aldol reactions with a high degree of asymmetric induction heralded a revolution in the field of organocatalysis, following a nearly 30 year hiatus since the report of the first proline-mediated transformation.² Organocatalysis has since become a fast growing area of research in organic chemistry, encompassing the discovery of new catalysts and new catalytic transformations.³ Mechanistic investigations have been slower to follow, although theoretical studies of proline-mediated transformations have provided significant insight.⁴ It is now commonly accepted that aldol and similar reactions proceed *via* enamine formation between proline and the donor substrate followed by attack on an electrophilic substrate, although no intermediates in the cycle have been isolated or directly observed.

Two examples in the panoply of efficient proline-mediated reactions may be singled out for their unusual kinetic features. We reported that the α -aminoxylation⁵ and α -amination⁶ of aldehydes (Scheme 1) exhibit autoinductive behaviour, *i.e.*, the reaction rate rises rather than falls as substrates are consumed during its course.⁷ This is



Scheme 1 Proline-mediated α -aminoxylation and α -amination.

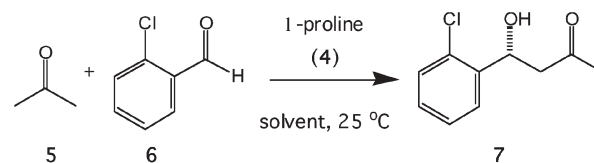
^a Department of Chemistry, Imperial College, London, UK SW7 2AZ. E-mail: d.blackmond@imperial.ac.uk; Fax: +44 (0)20 7594 5804; Tel: +44 (0)20 7594 1193

^b Department of Chemical Engineering and Chemical Technology, Imperial College, London, UK SW7 2AZ

† Electronic Supplementary Information (ESI) available: Further details of experimental procedures, compound characterisation, reaction conditions and theoretical calculations. See DOI: 10.1039/b609926b

‡ Present address: Mitsubishi Pharma Corporation, Kamisu, Ibaraki 314-0255, Japan.

§ Present address: Department of Chemistry, University of Calgary, 2500 University Drive NW, Alberta, Canada, T2N 1N4.



Scheme 2 Proline-mediated aldol reaction.

in contrast to aldol reactions (Scheme 2), which show conventional positive order kinetics in substrate concentration.⁸ Here, we present results of detailed kinetic studies that suggest a role for the product in the reactions of Scheme 1, adding to our fundamental mechanistic understanding of organocatalytic reactions in general.

Our initial experimental observations of a rising rate in proline-mediated α -aminoxylation and α -amination reactions were obtained using reaction calorimetry, which, as has been described previously,⁹ provides an accurate and virtually continuous measure of reaction rate as a function of time. The characteristic s-shaped temporal conversion profile expected for a reaction exhibiting an accelerating rate is shown in Fig. 1 for the α -amination carried out in DMF, a significantly more polar medium than the chlorinated hydrocarbon solvents used in earlier studies. Fig. 1 also shows that this rate acceleration is *not* observed in the aldol reaction of Scheme 2. This difference in the shape of the conversion profiles for the reaction of Scheme 1 compared to Scheme 2 was observed in all solvents we have tested, including CH_2Cl_2 , CHCl_3 , DMF, DMSO and CH_3CN .

An important consideration is the solubility of proline, which is low in most organic solvents. The rate increase observed in Fig. 1 might simply be attributed to an increase in the concentration of proline present in the active catalytic cycle, if undissolved proline becomes solubilised over the course of the reaction. However, this fails to explain why the aldol reaction does not show a similar accelerating rate behavior. This hypothesis may be tested if the reaction were studied under conditions of complete homogeneity in the reaction mixture. A number of recent studies have focused on the synthesis of proline derivatives or proline-inspired catalysts with an improved solubility in organic solvents for aldol and other transformations.^{8,10} We prepared compound **8** by derivatizing 4-hydroxyproline with $(\text{Pr})_2(\text{C}_8\text{H}_{17})\text{SiCl}$ (see the ESI†). **8** is completely soluble in CHCl_3 and other low dielectric solvents, even at temperatures as low as 0 °C. Fig. 2 compares the behavior of **8** as a catalyst in place of proline (**4**) in the α -aminoxylation reaction of Scheme 1 and the aldol reaction of Scheme 2, carried out in CHCl_3 . The kinetic profile of the α -aminoxylation reaction using **8** shows the s-shaped profile of an increasing rate, while aldol reactions carried out using **8** do not exhibit rate acceleration.

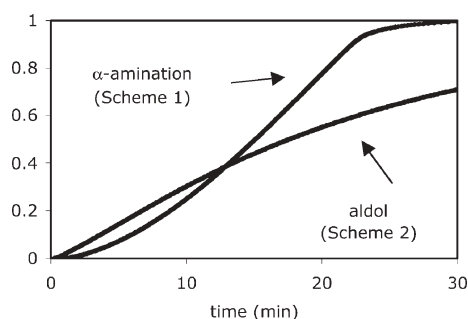


Fig. 1 Fraction conversion vs. reaction time for proline-mediated reactions in DMF. See the ESI for details.†

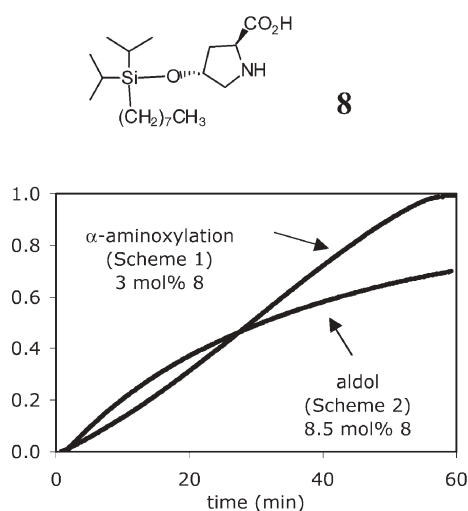


Fig. 2 Fraction conversion vs. time using soluble proline derivative **8** as the catalyst in CHCl_3 . See the ESI for details.†

Our results highlight a special feature of the reactions of Scheme 1 that cannot be rationalized simply by considering proline solubility. Quantitative kinetic analysis provides mechanistic evidence of a role for the reaction product in these reactions. A simple example of global reaction kinetics for a dual reaction pathway is described by eqn. 1, in which the rate of one pathway (I) depends on substrate and catalyst concentrations **1** and **4**, while a second pathway (II) also depends on product **3** concentration. As will be shown later, the reaction is zero-order with respect to **[2a]** or **[2b]**.

$$\text{total reaction rate} = r(\text{I}) + r(\text{II}) = (k_{\text{I}} \times [\text{1}] \times [\text{4}]) + (k_{\text{II}} \times [\text{1}] \times [\text{4}] \times [\text{3}]) \quad (1)$$

Complex rate behavior will be observed in cases where product acceleration is observed, because reaction rate initially increases as product **[3]** increases, but eventually must decrease as reactant **[1]** is fully consumed. The reaction progress kinetic profiles that are derived from these opposite contributions from substrate **[1]** and product **[3]** to the reaction rate may be deconvoluted by a simple algebraic manipulation of the rate law in eqn. 1 to give eqn. 2, which effectively normalizes the reaction rate at any given time by the concentration of reactant **1** at that time.

$$\frac{\text{total reaction rate}}{[\text{1}]} = \frac{r(\text{I}) + r(\text{II})}{[\text{1}]} = (k_{\text{I}} \times [\text{4}]) + (k_{\text{II}} \times [\text{4}] \times [\text{3}]) \quad (2)$$

A large number of data points may be obtained over the course of a reaction *via* reaction progress measurements, with each point

describing a unique condition of (rate, **[1]**, **[3]**, time). We may use these data to construct plots in the form of eqn. 2, where the function on the left-hand side of the equality sign (rate/[**1**]) is plotted on the y-axis and **[3]** is plotted on the x-axis. Eqn. 2 has the form of a straight line with a gradient = $k_{\text{II}} \times [\text{4}]$ and y-intercept = $k_{\text{I}} \times [\text{4}]$. Thus, the slope provides information about the kinetics of the product-assisted pathway II, while the y-intercept relates to the kinetics of the conventional pathway I. Fig. 3 shows plots of this “graphical rate equation” using reaction progress data from reaction calorimetric monitoring of the reactions of Scheme 1 (α -aminoxylation, Fig. 3a; α -amination, Fig. 3b), carried out with different initial concentrations of reactants **1** and either **2a** or **2b**. As has been discussed previously,⁹ such plots can yield several important pieces of information. Firstly, when reaction progress rate profiles, normalized by a substrate concentration, fall on top of one another (“overlay”) for reactions carried out at different “excess” values,¹¹ this overlay demonstrates that the reaction follows first-order kinetics in the “normalized” substrate concentration (**1** in this example). Secondly, the positive linear gradient of the plots demonstrates first-order kinetics in the concentration of the species plotted on the x-axis (product **3a** or **3b** in this case). In addition, the overlay between runs carried out at different concentrations of electrophile **2a** or **2b** confirms that the reaction is zero-order with respect to electrophile concentration. The relative contributions of pathways I and II depend on **[3]**, and may be determined from the ratio of the slope and the intercept of plots in Fig. 3, as seen in eqn. 3. The data in Fig. 3 show that pathway II contributes more to the overall rate for the α -aminoxylation reaction than it does for the α -amination.

$$\frac{\text{reaction rate (II)}}{\text{reaction rate (I)}} = \frac{\text{slope} \times [\text{3}]}{\text{intercept}} \quad (3)$$

A point that is not illustrated explicitly in Fig. 3 is that reactions carried out at different concentrations **[1]** require significantly different times for completion. For example, reaction at the lowest **[1]** in Fig. 3b requires nearly twice as long for complete conversion as those at the highest **[1]** (see the ESI†), yet they bear the same kinetic relationship to instantaneous product concentration. This confirms that the relationship indicated by the “overlay” of curves is a function of *reaction stoichiometry* and not simply a temporal relationship, as might be expected if the autoinductive behavior was related to dynamic processes unrelated to the catalytic network.

These observations suggest that the product is associated with the catalyst in the rate-limiting step of pathway II. One possible

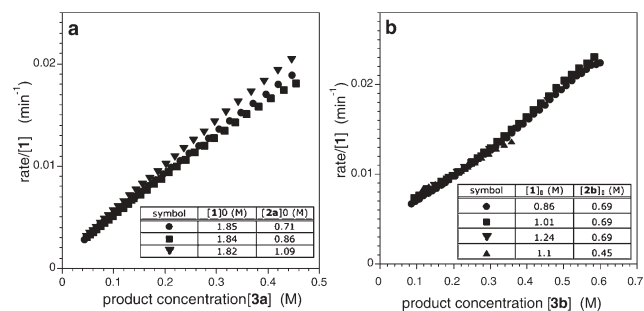
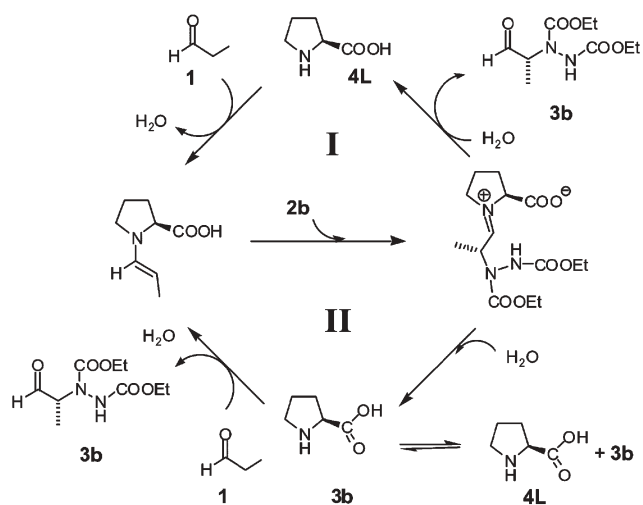


Fig. 3 Graphical rate equation of rate/[aldehyde] vs. [product] according to eqn. 2 for the reactions of Scheme 1. (a) α -Aminoxylation at 5 °C in CHCl_3 , 0.07 M **4**. (b) α -Amination at 10 °C in CH_2Cl_2 , 0.14 M **4**.



Scheme 3 Parallel catalytic cycles for reactions of Scheme 1.

mechanism consistent with these data is shown in Scheme 3, illustrated for the example of α -amination. This proposes that a product–proline adduct is reversibly formed in Pathway II, with rate-limiting addition of the aldehyde occurring prior to full dissociation of the reaction product. This product-assisted cycle could exist in parallel with the conventional catalytic cycle that has been proposed for proline-mediated aldol reactions, shown in I on the top of Scheme 3. As the reactions of Scheme 1 proceed, product–proline-binding channels a greater fraction of the proline into this product-assisted cycle, and the higher reactivity of it results in a concomitant increase in rate. Product stereochemistry is determined in steps common to cycles I and II.

While the kinetic data support the role of a product–proline adduct in the catalytic cycle, as shown in Scheme 3, these data cannot provide further information about the nature of such a species. We proposed previously, on the basis of computational evidence, that this species is a hydrogen bonded adduct.¹² The question of why reactant **1** might add more readily to proline as it is releasing the hydrogen bound product than it does to free proline may be addressed using theoretical calculations of the electrostatic potential near to the van der Waals surface of two proline conformations obtained *via* DFT calculations using B3LYP/6-31G(d) (see the ESI†). One globally optimal “closed” conformation is shown in Fig. 4A, with the lone pair on N providing a hydrogen bonding attachment point for the carboxylic proton, causing proline to fold in on itself such that **A** is not optimally positioned for the Brønsted acid-assisted nucleophilic attack that characterizes proline’s reaction with carbonyl groups.¹³ Structure Fig. 4B is an “open” proline conformation, similar to those used in other theoretical studies as the starting point for probing interactions between proline and aldehydes or ketones.¹⁴ A hydrogen bonded product–proline complex will resemble conformation **B** rather than the more stable conformation **A**. If association of aldehyde to this complex commences prior to full product dissociation, the catalyst may be maintained in its active conformation from one cycle to the next. In the non-product-assisted pathway, proline readily reverts to the more stable conformation **A**, meaning that a significant reactivation energy cost is incurred with each cycle.

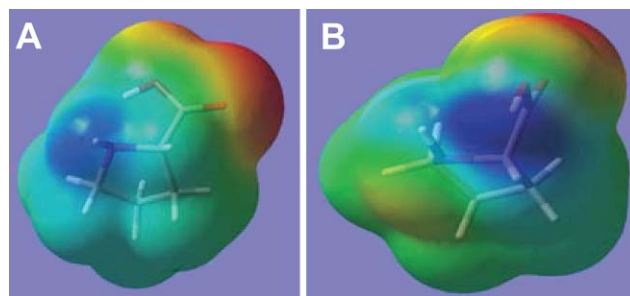


Fig. 4 Electrostatic potential near to the van der Waals surface for “closed” (A) and “open” (B) proline; see the ESI†

The importance of hydrogen bond mediation in asymmetric catalysis has been highlighted recently.¹⁵ A reaction product that uses hydrogen bonding to enable higher efficiency in its own catalytic production suggests a tool for the evolutionary development of primitive amino acid catalysts and provides a mechanistic rationale that may help in the design of new organocatalysts.

Notes and references

- B. List, R. A. Lerner and C. F. Barbas, III, *J. Am. Chem. Soc.*, 2000, **122**, 2395.
- (a) Z. G. Hajos and D. R. Parrish, *J. Org. Chem.*, 1974, **39**, 1615; (b) U. Eder, G. Sauer and R. Wiechert, *Angew. Chem., Int. Ed. Engl.*, 1971, **10**, 496.
- (a) P. I. Dalko and L. Moisan, *Angew. Chem., Int. Ed.*, 2004, **43**, 5138; (b) J. Seayad and B. List, *Org. Biomol. Chem.*, 2005, **3**, 719; (c) H. Gröger and J. Wilken, *Angew. Chem., Int. Ed.*, 2001, **40**, 529; (d) B. List, *Acc. Chem. Res.*, 2004, **37**, 548.
- C. Allemann, R. Gordillo, F. R. Clemente, P. H.-Y. Cheong and K. N. Houk, *Acc. Chem. Res.*, 2004, **37**, 558.
- (a) G. Zhong, *Angew. Chem., Int. Ed.*, 2003, **42**, 4247; (b) S. P. Brown, M. P. Brochu, C. J. Sinz and D. W. C. MacMillan, *J. Am. Chem. Soc.*, 2003, **125**, 10808.
- (a) B. List, *J. Am. Chem. Soc.*, 2002, **124**, 5656; (b) N. Kumaragurubaran, K. Juhl, W. Zhuang, A. Bøgevig and K. A. Jørgensen, *J. Am. Chem. Soc.*, 2002, **124**, 6254.
- (a) S. P. Mathew, H. Iwamura and D. G. Blackmond, *Angew. Chem., Int. Ed.*, 2004, **43**, 2099; (b) H. Iwamura, S. P. Mathew and D. G. Blackmond, *J. Am. Chem. Soc.*, 2004, **126**, 11770.
- A. Hartikka and P. I. Arvidsson, *Tetrahedron: Asymmetry*, 2004, **15**, 1831.
- (a) D. G. Blackmond, *Angew. Chem., Int. Ed.*, 2005, **44**, 4302; (b) J. S. Mathew, M. Klussmann, H. Iwamura, F. Valera, A. Futran, E. A. C. Emanuelsson and D. G. Blackmond, *J. Org. Chem.*, 2006, **71**, 4711.
- (a) H. Torii, M. Nakadai, K. Ishihara, S. Saito and H. Yamamoto, *Angew. Chem., Int. Ed.*, 2004, **43**, 1983; (b) A. J. A. Cobb, D. M. Shaw and S. V. Ley, *Synlett*, 2004, 558; (c) A. Berkessel, B. Koch and J. Lex, *Adv. Synth. Catal.*, 2004, **346**, 1141; (d) Y. Hayashi, J. Yamaguchi, K. Hibino, T. Sumiya, T. Urushima, M. Shoji, D. Hashizume and H. Koshinob, *Adv. Synth. Catal.*, 2004, **346**, 1435; (e) A. J. A. Cobb, D. M. Shaw, D. A. Longbottom, J. B. Gold and S. V. Ley, *Org. Biomol. Chem.*, 2005, **3**, 84.
- “Excess” = difference between substrate concentrations = $[2]_0 - [1]_0$.
- H. Iwamura, D. H. Wells, Jr., S. P. Mathew, M. Klussmann, A. Armstrong and D. G. Blackmond, *J. Am. Chem. Soc.*, 2004, **126**, 16312.
- Stable “closed” forms exist with the carboxyl O-atoms in the “Z” configuration, leaving the N-lone pair free for attack, but making the carboxylic proton unavailable as a co-catalyst. We thank D. A. Singleton for a personal communication concerning this point.
- K. N. Rankin and J. W. Gault, *J. Phys. Chem. A*, 2002, **106**, 5155.
- (a) M. S. Taylor and E. N. Jacobsen, *Angew. Chem., Int. Ed.*, 2006, **45**, 1520; (b) P. R. Schreiner, *Chem. Soc. Rev.*, 2003, **32**, 289; (c) A. I. Nyberg, A. Usano and P. M. Pihko, *Synlett*, 2004, 1891.